Formation of active cu-oxo clusters for methane oxidation in cu-exchanged mordenite

Ikuno, Takaaki; Grundner, Sebastian; Jentys, Andreas; Li, Guanna; Pidko, Evgeny; Fulton, John; Sanchez-Sanchez, Maricruz; Lercher, Johannes A.

DOI
10.1021/acs.jpcc.8b10293

Publication date
2019

Document Version
Final published version

Published in
Journal of Physical Chemistry C

THE JOURNAL OF PHYSICAL CHEMISTRY C

Article

Cite This: J. Phys. Chem. C 2019, 123, 8759−8769

pubs.acs.org/JPCC

Formation of Active Cu-oxo Clusters for Methane Oxidation in Cu-Exchanged Mordenite

Takaaki Ikuno,[†] Sebastian Grundner,[†] Andreas Jentys,[†] Guanna Li,[‡] Evgeny Pidko,[‡] John Fulton,[§] Maricruz Sanchez-Sanchez,*[,†] and Johannes A. Lercher*[,†,§]

[†]Department of Chemistry and Catalysis Research Institute, TU München, Lichtenbergstrasse 4, 85748 Garching, Germany

[‡]Department Chemical Engineering, Delft University of Technology, Van der Maasweg 9, Delft 2629 HZ, The Netherlands

[§]Institute for Integrated Catalysis, Pacific Northwest National Laboratory, P.O. Box 999, Richland, Washington 99352, United States

Supporting Information

ABSTRACT: Cu-exchanged zeolites are known to be active in the selective oxidation of methane to methanol at moderate temperatures. Among them, Cu-exchanged mordenite (MOR) is the system that has so far shown the highest methanol yield per Cu atom. This high efficiency is attributed to the ability of MOR to selectively stabilize an active tricopper cluster with a $[Cu_3(\mu\text{-}O)_3]^{2+}$ structure when activated in the presence of O_2 at high temperatures. In this study, we investigate the elementary steps in the formation of $[Cu_3(\mu\text{-}O)_3]^{2+}$ by in situ X-ray absorption spectroscopy and ultraviolet−visible spectroscopy. We demonstrate that the Cu cations undergo a series of thermally driven steps during activation that precede the formation of the active oxidizing species. We hypothesize that the thermal formation of highly mobile Cu^+ species by autoreduction of Cu^{2+} in an inert gas is essential to enable the reorganization of Cu ions in MOR, which is necessary for the formation of a reduced precursor of $[Cu_3(\mu\text{-}O)_3]^{2+}$. Such a precursor can be oxidized in the presence of strong oxidants—such as O_2 and N_2O—to form active $[Cu_3(\mu\text{-}O)_3]^{2+}$ at temperatures as low as 50 °C.

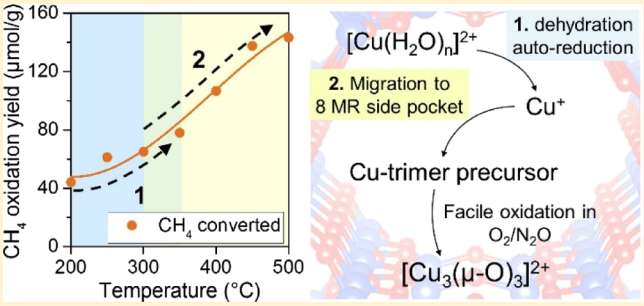

1. INTRODUCTION

Direct conversion of methane to methanol at moderate temperatures has been attracting enormous attention because of the increasing availability of methane and its local dispersion as well as the importance of methanol as a chemical feedstock and as an energy source.[1] However, the high stability of CH_4 in comparison to any of its partial oxidation products makes it challenging to achieve high selectivities to methanol at significant conversions.

In nature, methane monooxygenase enzymes in methanotrophic bacteria are able to convert methane to methanol under aerobic conditions at Cu- and Fe-active centers.[2−4] Inspired by these enzymes, Cu-[5−9] and Fe-exchanged zeolites[9−12] have been studied extensively as inorganic biomimetic catalysts. Because of their crystallinity, framework negativity, and microporosity, zeolites provide a highly confined environment to host small metal and metal-oxide clusters in an ordered and controlled way.[7,13−17]

Studies on Fe-zeolites have shown that the active site precursor in the catalyst has to be oxidized using N_2O to form $Fe(III)-O^{\bullet-}$ species, which are concluded to be able to activate methane via highly active radical oxygen species.[10,11,18] However, methane oxidation with molecular O_2, which is more economical than N_2O, has not been achieved on Fe-zeolites. Conversely, Cu-exchanged zeolites have shown activity in the partial oxidation of methane to methanol with small concentrations of O_2[6,8,19−26] as well as with N_2O[24,25,27,28] or NO.[20] It should be noted that in all cases, methane oxidation to methanol is carried out in three separated stages. First, the catalyst has to be activated at high temperatures (450−600 °C) to form active Cu-oxo species. Then, at lower temperatures, typically 150−250 °C, CH_4 reacts on the activated material via hydrogen abstraction, resulting in an intermediate that is strongly adsorbed on the active sites.[29] To desorb the oxidized product as methanol, it is necessary to aid desorption by adding H_2O or by extraction in polar solvents. Once methanol is extracted, the catalyst must undergo thermal activation again at 450−600 °C to regenerate the active Cu species and remove the polar solvent from the zeolite. Under these three-stage reaction conditions, Cu trimer[7,24,30,31] and Cu dimers[6,15,19,26,27,32−35] have been reported as active species. The continuous oxidation of methane to methanol on Cu-zeolite catalysts in the presence of gas-phase H_2O using O_2[8] or N_2O[28] as an oxidant has been reported, although limited to very low turnovers.

Received: October 22, 2018
Revised: March 11, 2019
Published: March 18, 2019

DOI: 10.1021/acs.jpcc.8b10293
J. Phys. Chem. C 2019, 123, 8759−8769

The highest temperature of the three-stage methane oxidation process is typically needed for the oxidative activation of the catalysts, rather than for methane reaction or methanol extraction steps. In general, activation temperatures lower than 450 °C seem to lead consistently to a significant reduction in the activity of the catalysts.[6−8,20,25,36−38] Therefore, it seems highly important to understand the formation and regeneration of Cu-active species in zeolite frameworks to achieve higher methanol yields.

The chemical processes during the synthesis of Cu-zeolite catalysts, ranging from the Cu-ion exchange step to thermal activation, determine the final speciation of Cu species in a particular framework.[7,24,25,35,39−44] Water ligands coordinated to Cu^{2+} ions—located in the zeolite cavities after the ion-exchange step—are removed during thermal treatment. During this process, Cu^{2+} ions move toward their final exchange positions in the zeolite, which are closer to the negative charges at Al-substituted T-sites.[40,44−46] The generation of monovalent $[Cu-OH]^+$ species attached to framework Al sites has also been proposed to occur in this step.[25,42,43,47] Such species have the potential to generate multinuclear Cu-oxo clusters via condensation with adjacent $[Cu-OH]^+$ and formation of a μ-oxo bridge between Cu^{2+} cations.[48−50] The activation of methane at low temperatures is attributed to this μ-oxo species bridging two Cu^{2+}.[7,26,32−34,41] Therefore, the processes of formation and decomposition of this moiety are relevant to the synthesis of efficient Cu-zeolite catalysts.

Apart from the removal of water ligands during the thermal treatment performed at temperatures above 350 °C in an inert atmosphere, autoreduction of Cu^{2+} to Cu^+ has been observed.[26,44,50−53] This autoreduction process is supposed to occur via recombination and desorption of the bridging O of μ-oxo-bridged Cu species as O_2.[43,49,54,55]

Pappas et al. studied the dehydration and oxidation of Cu species in the Chabazite (CHA) framework and their effect on Cu speciation and activity in methane oxidation.[25] They attributed the lower activity of Cu-SSZ-13 oxidized at mild temperatures to differences in the Cu−O coordination structure formed during the activation under different conditions. Differences in the activity of O_2- and N_2O-activated Cu-mordenite (MOR) catalysts were reported by Kim et al.[24] They attributed the higher activity obtained with N_2O to the lower negative change in entropy during activation in N_2O compared to O_2 and, in addition, to the necessary O−O cleavage of an intermediate species when O_2 is used as the oxidant. Recent theoretical studies have also tackled both the generation and activity of $[CuOCu]^{2+}$ and $[Cu_3(\mu\text{-}O)_3]^{2+}$ species in MOR.[56,57]

Despite all these studies, it is still unclear why is it necessary to activate the catalyst at temperatures above 400 °C to achieve full activity. A better understanding of the formation of active Cu-oxo clusters and its kinetically or thermodynamically limiting steps is required to develop more efficient methane oxidation catalysts.

In this work, we investigate the formation of Cu-oxo species in a highly active Cu-MOR catalyst that was developed in our laboratories.[7] This material has been shown to contain only a tricopper-oxo cluster as active species when activated in O_2 at 450−500 °C.[7] The processes of dehydration, autoreduction, and oxidation of Cu species in MOR were monitored in detail by in situ spectroscopies, and the activity in methane oxidation was correspondingly tested under various conditions. The mobility of auto-reduced Cu^+ species at high temperature was found to be a crucial factor in the formation of active Cu-oxo clusters.

2. EXPERIMENTAL METHODS

2.1. Preparation of the Cu-MOR Catalyst. Parent H-MOR was obtained by the calcination of a commercial NH_4-MOR (Clariant, Si/Al = 11) in synthetic air (100 mL/min) at 550 °C for 6 h. The Cu-MOR catalyst was prepared by ion-exchange of H-MOR in an aqueous solution of $Cu(CH_3COO)_2$ at an ambient temperature using 60 mL/$g_{zeolite}$ of 0.01 M precursor solution. The pH of the solution was adjusted to 5.7 by adding HNO_3 prior to the addition of H-MOR. After the exchange, the solid phase was collected by centrifugation and rinsed by redispersion in water (50 mL/$g_{zeolite}$), followed by centrifugation. The rinsing step was repeated four times, and the sample was dried at 100 °C for 24 h. These ion-exchange conditions have been previously adjusted to avoid precipitation of Cu-oxo species,[30] and therefore, formation of significant concentrations of CuO or $Cu(OH)_2$ is excluded (see Table S2 in the Supporting Information).

2.2. Selective Oxidation of Methane to Methanol. CH_4 oxidation activity of the Cu-MOR catalyst (50 mg) was tested under ambient pressure in a stainless steel plug flow reactor with 4 mm inner diameter. The catalyst was pressed and sieved to the particle size of 250−400 μm. In the typical reaction testing, the catalyst was first activated in pure O_2 (16 mL/min) at 500 °C for 1 h. After cooling down to 200 °C in O_2, the catalyst was purged in He, and CH_4 loading was performed for 4 h in 90% CH_4 in He (16 mL/min). The catalyst was subsequently cooled down to 135 °C in He, and H_2O steam-assisted product desorption was performed for 30 min in 50% H_2O in He (20 mL/min). The reaction products were identified and quantified by online mass spectrometry [m/z 31, 44, and 46 for CH_3OH, CO_2, and $(CH_3)_2O$, respectively]. $(CH_3)_2O$ was regarded as a product that stems from the condensation of two CH_3OH molecules and therefore considered as a CH_3OH equivalent. The sum of all detected products was defined as the total yield of methane oxidation products.

2.3. In Situ X-ray Absorption Spectroscopy. X-ray absorption spectra were recorded on beamline P65 at PETRA III of DESY in Hamburg, Germany. The electron energy was 6 GeV with a beam current of 100 mA. The beam size at the sample was 200 × 300 μm. Around 10 mg of the sample was sandwiched between quartz wools and packed in a quartz capillary reactor (1 mm outer diameter and 0.02 mm wall thickness) and placed on top of a gas blower for controlled heating. A double-crystal Si(111) monochromator was used to control the incident photon energy, and the spectra were recorded with ionization chamber detectors in the transmission mode. To suppress higher harmonics in the incident beam, the monochromator was detuned to 70% of the maximum peak intensity. Thermal activation of the samples was performed in a flow of 10% O_2 in He as well as in He at 5 mL/min at 450 °C for 1 h with the 10 °C/min heating rate. After the thermal activation of the sample in He at 450 °C, the sample was cooled down to 200 °C in a He flow and treated in a flow of 10% O_2 in He for 30 min. The gas flow over the samples was controlled by mass-flow controllers. A moisture/oxygen trap and a moisture trap were employed on He and O_2 gases, respectively, to avoid unwanted contamination of the gas

DOI: 10.1021/acs.jpcc.8b10293
J. Phys. Chem. C 2019, 123, 8759−8769

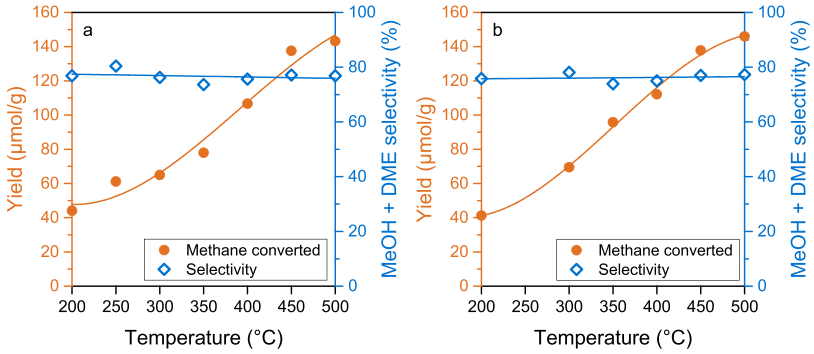

Figure 1. Comparison of the activity and selectivity of Cu-MOR with a Cu loading of 420 μmol g^{-1} after activation in (a) pure O_2 and (b) N_2O at various temperatures. Methane loading was performed at 200 °C in 90% CH_4 for 4 h.

stream on the catalyst. X-ray absorption near edge structure (XANES) and extended X-ray absorption fine structure (EXAFS) data processing were performed on Athena software from the Demeter package.[58]

2.4. In Situ Ultraviolet−Visible Spectroscopy. Measurements of ultraviolet−visible (UV−vis) spectra of the Cu-MOR catalyst were carried out on an Avantes AvaSpec 2048 spectrometer equipped with a high-temperature optical fiber (Avantes FCR-7UV400-2ME-HTX). The sample (250−400 μm particle size) was placed in a quartz flow reactor with square optical-grade quartz windows. The intensity of the diffuse reflectance UV−vis is shown as the Kubelka−Munk function, defined as $F(R) = (1 - R)^2/2R$, where $R = R_s/R_r$. R_s and R_r refer to the signal intensity of the sample and reference, respectively. Parent H-MOR was used as the reference. The catalyst was first treated in a N_2 flow (16 mL/min) at 450 °C for 1 h and then cooled down to 200 °C. Then, the catalyst was contacted with the O_2 flow (16 mL/min) for 30 min at 200 °C, followed by flushing in N_2 and subsequent contact with the CH_4 flow (16 mL/min) for 1 h.

2.5. Density Functional Theory Calculation. Spin-polarized density functional theory (DFT) calculations were performed using VASP 5.3.5.[59,60] The Perdew−Burke−Ernzerhof functional based on the generalized gradient approximation was chosen to account for the exchange−correlation energy.[61] A plane-wave basis set in combination with the projected augmented wave method was used to describe the valence electrons and the valence−core interactions, respectively.[60] The kinetic energy cutoff of the plane-wave basis set was 400 eV. Gaussian smearing of the population of partial occupancies with a width of 0.05 eV was used. The threshold for energy convergence for each iteration was set to 10^{-5} eV. Geometries were assumed to be converged when forces on each atom were less than 0.05 eV/Å. Considering the large unit cell, Brillouin zone-sampling was restricted to the gamma point. The supercell of the all-silica MOR framework was constructed by doubling the monoclinic primary unit cell along the *c*-axis.[62] The positive charge of the extra framework Cu-containing clusters is compensated by the Al pair located in the 12-membered ring at the mouth of the side pocket.[7]

3. RESULTS AND DISCUSSION

3.1. Impact of Activation Temperature and Oxidant on the Activity of Cu-MOR. Activity tests of Cu-MOR in methane oxidation after activation under different conditions were performed in a typical three-stage reaction, as described elsewhere[7] and in the Experimental Methods section. Briefly, unless stated, methane is allowed to react for 4 h in all experiments performed in this work. The long reaction time allows for a complete titration of all sites active for methane activation. In this way, quantification of the methane oxidation products yields quantitative information of the active site concentration in Cu-MOR.[7]

To study the impact of activation temperature on the methane oxidation activity, the freshly prepared sample was activated in pure O_2 for 1 h at different temperatures, subsequently cooled to 200 °C in O_2, and then flushed with He at the reaction temperature, before it was contacted with methane. A significant increase in activity with increasing temperature of activation was observed from 200 to 450 °C before it leveled off at 450−500 °C (Figure 1a). The structure of Cu-active sites for the sample treated at 450−500 °C is a tricopper-oxo cluster (Cu_3O_3).[7] We would like to mention that only a minimal concentration of Cu spectators was formed when activation was performed at 450−500 °C.[7] Thus, the high activity of Cu-MOR activated at 450−500 °C is attributed to the high concentration of Cu species forming active sites. It should be noted, however, that for activation temperatures as low as 200 °C, about 30% of the maximum methane oxidation yield is reached. This lower activity is hypothesized to result from an incomplete formation of $(Cu_3O_3)^{2+}$-active sites or from the formation of different active species such as water-stable Cu^{II}-oxide species.[41] However, the constant selectivity over the whole temperature range strongly points to a gradual increase in the concentration of one structurally well-defined type of active Cu species with activation temperature. Ab initio calculations have shown that $[Cu_3(\mu\text{-}O)_3]^{2+}$ is thermodynamically the most stable species at low H_2O partial pressures.[7] Infrared (IR) spectra of the Cu-MOR sample were recorded at different temperatures in the O_2 flow (Figure S1 in the Supporting Information). The spectra show a band at 3610 cm^{-1}, attributed to Brønsted acid sites of the zeolite, already at 200 °C. This indicates that, although dehydration of zeolite is not complete, local H_2O concentration in at least some regions is low enough to allow the formation of $[Cu_3(\mu\text{-}O)_3]^{2+}$ species. Hence, it is hypothesized that the formation of active sites is either kinetically or thermodynamically limited at temperatures below 450 °C, and only a fraction of Cu reaches the configuration that is able to activate methane.

Prolonging the duration of the activation step in pure O_2 from 1 to 3 h at 350 and 500 °C resulted in the increment of activity of only 6.5 and 3.3%, respectively, whereas the

DOI: 10.1021/acs.jpcc.8b10293
J. Phys. Chem. C 2019, 123, 8759−8769

selectivity to methanol was maintained in the range of 70−77% (Figure S2). Thus, we conclude that the formation of active Cu species is mostly thermodynamically controlled in the temperature range of 350−500 °C, and the increase in the activity observed in Figure 1a is mainly due to increasing concentrations of the active sites, with the maximum concentration achieved at 450 °C. It should be noted that in the case of the Cu-CHA catalyst, it has been reported that prolonging the activation time from 1 to 2 and 8 h at 450 °C increased the activity of the catalyst by ca. 25% and ca. 100%, respectively.[25] This different behavior is a first indication of the strong impact of the zeolite framework structure on the processes leading to Cu speciation in the micropores.

In the next step, oxidative activation of Cu-MOR was studied using two different types of oxidants: O_2 and N_2O. It is widely accepted that μ-oxo bridges connecting Cu ions activate methane.[7,34,63] In O_2, the formation of μ-oxo bridges (as well as the subsequent insertion of an O atom in methane to produce methanol) requires O−O bond cleavage. This implies the migration of the second O atom in the zeolite pores and its subsequent recombination to O_2 or, alternatively, the formation of another μ-oxo bridge between available Cu ions. Conversely, N_2O can readily provide one oxygen atom to a Cu site, releasing N_2. Thus, differences between the activity after O_2 and N_2O activations would allow to detect if the oxidative activation is a limiting process for Cu-MOR.

Methane activation was performed on the same Cu-MOR catalyst activated at different temperatures in O_2 and N_2O (Figure 1a,b). Both activity and selectivity of Cu-MOR after activation at 200−500 °C in O_2 and N_2O were similar, even though small differences can be noticed in the activation temperature range of 300−400 °C. The identical maximum yield of ca. 140 μmol/g of converted methane was achieved with both oxidants at temperatures of activation of 450−500 °C. This maximum yield corresponds to a stoichiometry of approximately one CH_4 molecule activated per three Cu atoms. Thus, we conclude that the formation of active Cu-oxo species—in particular tricopper oxo clusters—is complete after activation at 450−500 °C both in O_2 and in N_2O. The nearly identical activity and selectivity when activated either in O_2 or N_2O (Figure 1) shows also that the O−O bond cleavage in the oxidation by O_2 does not limit the formation of active Cu species in the zeolite under the conditions studied here.

It should be noted that a similar study by Kim et al. reported significantly higher activities (2−3 times higher) for Cu-MOR activated at 300−350 °C in N_2O in comparison to activation in O_2. They attributed this behavior to the higher enthalpy release of the formation of Cu(II) oxide with N_2O (82 kJ/mol more exothermic than with O_2 under standard conditions).[24] However, the oxidations of Cu^+ to Cu^{2+} in N_2O and O_2 are both thermodynamically favored under the conditions studied here; therefore, we do not expect that this enthalpy difference would have a remarkable impact on the formation of active Cu-oxo species. Kim et al.[24] also suggested that the lower activity of the O_2-activated catalyst when treated at 500−600 °C is because the formation of an intermediate species is hampered at high temperatures.[64] On the contrary, we did not observe a difference in the CH_4 oxidation activity between N_2O- and O_2-activated catalysts.

3.2. Elementary Steps in the Activation of Cu-MOR Catalysts. To obtain deeper insight into the elementary steps involved in the oxidative activation of Cu species in MOR, it is necessary to decouple the (re)oxidation of Cu from other thermally driven processes taking place during the high-temperature activation, such as dehydration of the zeolite. Thus, we activated Cu-MOR, first in a He flow at 500 °C for 1 h and then in 5% O_2/He for 10 min at temperatures ranging from 50 to 200 °C. Even though oxidation conditions in terms of oxidant concentration and temperature were much milder than in the standard procedure, Cu-MOR converted a similar amount of CH_4 (Figure 2). Thermal activation of Cu-MOR in

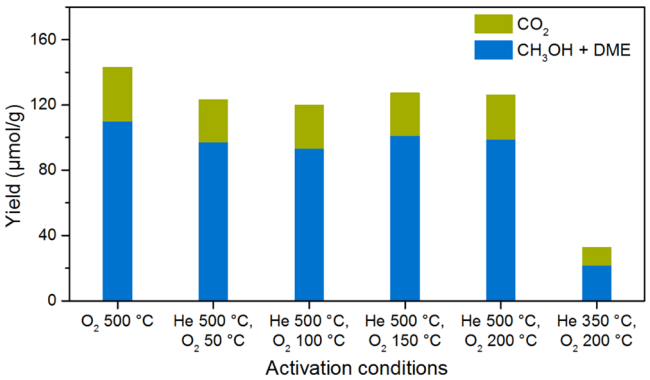

Figure 2. Activity and selectivity of Cu-MOR (Cu loading of 420 μmol g^{-1}) after activation in O_2 at 500 °C and after activation in He for 1 h and subsequent oxidation in 5% O_2 at various temperatures for 10 min. Methane loading was performed at 200 °C in 90% CH_4 for 4 h.

He and the subsequent low-temperature oxidation in N_2O also led to a similar conversion and selectivity (Figure S3). As a reference, Cu-MOR was activated in He at 500 °C without the subsequent O_2/N_2O step, and this catalyst showed only 10% of the full activity. This indicates that (re)oxidation of the Cu species is required for developing activity in methane conversion to methanol. On the other hand, when the Cu-MOR catalyst was activated in He at moderate temperatures (350 °C) and subsequently oxidized in O_2 at 200 °C, it showed only 23% of the full activity obtained by thermal activation in O_2 at 500 °C (Figure 2). Therefore, we conclude that the maximum concentration of active sites in Cu-MOR is produced upon contact with O_2 (or N_2O) as long as the material has been previously thermally treated at 450−500 °C.

It should be noted that similar experiments performed on Cu-SSZ-13 catalysts (i.e., oxidation in O_2 at 200 °C after thermal activation in He at 500 °C) resulted in 45% lower activity compared to thermal activation in O_2 at 500 °C.[25] This was attributed to a different speciation of Cu. The difference between zeolites convincingly shows that the nature of the framework plays an important role in the type of active Cu species stabilized under different conditions.

Our activity results shown in Figures 1 and 2 and Figure S2 in the Supporting Information suggest that the temperature dependence of the activation step is related to the formation of a Cu cluster precursor, which requires high temperatures. Such a precursor can be easily oxidized (even at low temperatures) by both N_2O and O_2, and it rapidly forms the active species responsible for methane activation.

3.3. In Situ Spectroscopy of Cu-MOR Activation. The redox chemistry of Cu embedded in zeolites during activation was monitored by in situ X-ray absorption spectroscopy (XAS) and UV−vis spectroscopy.

First, oxidative activation under standard conditions (pure O_2 atmosphere, 450 °C, 1 h) was studied by in situ XAS.

DOI: 10.1021/acs.jpcc.8b10293
J. Phys. Chem. C 2019, 123, 8759−8769

Figure 3 shows the Cu K-edge XANES of Cu-MOR during the heating stage and after the activation treatment. The presence of a weak pre-edge feature at 8978 eV, because of the 1s → 3d transition of Cu^{2+}, indicates the dominant Cu^{2+} character of all spectra taken along the activation process. The rising edge feature at 8987 eV, assigned to the 1s → 4p transition of Cu^{2+}, is attributed to a change in the coordination geometry of Cu^{2+} because of the loss of ligated water and an increasing interaction with the zeolite framework during thermal treatment.[32] The loss in intensity of the maximum absorption feature at 8997 eV with increasing temperature is indicative of the removal of water ligands[41] and indicates that the dehydration of the octahedral Cu^{2+} complexes in the pores leads to framework-coordinated Cu^{2+} species. The white line intensity at 8997 eV did not change at temperatures above 350 °C, revealing that dehydration of the Cu^{2+} centers is already complete at this temperature.

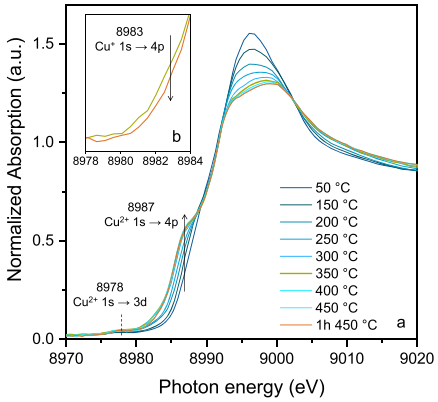

Figure 3. (a) Cu K-edge XANES of Cu-MOR during thermal activation in O_2 and (b) comparison of the Cu(I) feature at 8983−8984 eV after activation at 350 and 450 °C.

Comparison of the XANES recorded during activation at 350 °C with the spectra after activation at 450 °C for 1 h (Figure 3b) showed a feature at 8983 eV attributed to the 1s → 4p transition of Cu^{+} at 350 °C, which disappears on increasing the temperature to 450 °C. Hence, we hypothesize that a small fraction of Cu (ca. 5%) is reduced to Cu^{+} during the heating ramp even in the presence of O_2.

The state of Cu during thermal activation of Cu-MOR in an inert atmosphere was followed by XANES. Figure 4 shows the XANES recorded while heating the fresh sample in He to 450 °C. Similar to activation in O_2, the intensity of the peak at 8997 eV decreased with increasing temperature and reached an almost constant intensity at 350 °C, indicating that dehydration of Cu^{2+} species is largely complete at 350 °C. The most characteristic change during activation in He was the emergence of a pronounced absorption at 8984 eV, which is attributed to the 1s → 4p transition of Cu^{+}. At 350 °C, this feature corresponded to approximately 60% of the total reducible Cu, that is, the Cu population that underwent autoreduction in He at 450 °C. Because dehydration was completed at 350 °C, the Cu^{2+} → Cu^{+} reduction was the dominant reaction in the range of 350−450 °C.

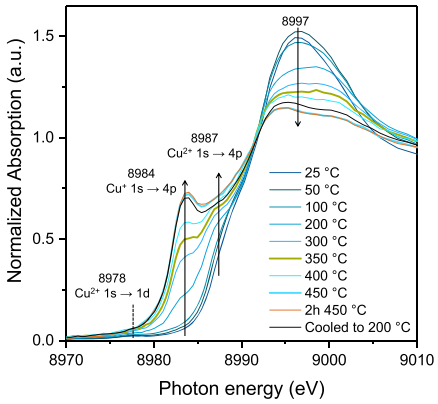

Figure 4. Cu K-edge XANES of Cu-MOR during thermal activation in He.

The autoreduction of Cu^{2+} to Cu^{+} during thermal treatment in an inert atmosphere has been widely reported.[35,42,43,50,55,65−69] The most widely proposed mechanism is the desorption of an O radical from μ-oxo-bridged Cu^{2+} followed by the subsequent recombination to O_2.[35,47−49] It has also been suggested that Cu^{+} is formed via the loss of a −OH ligand from $[CuOH]^{+}$-exchanged species, resulting in a Cu^{+} species coordinated to an Al-site.[42,50] The different pathways are hypothesized to be caused by different Cu species, that is, a single Cu^{2+} coordinated to two Al tetrahedra cannot be autoreduced by oxygen desorption under the described conditions.[25]

The autoreduction of exchanged Cu^{2+} appears to be favored[70] because even in the presence of O_2, reduction of a fraction of Cu^{2+} to Cu^{+} was detected by XANES (Figure 3), which is in good agreement with the literature.[24,71]

The radial distribution function (rdf) of the coordination structure around Cu during activation probed by EXAFS is compiled in Figure 5. The most prominent peak was observed below 2 Å in the *R*-space and is associated with backscattering from oxygen directly linked to Cu. The features above 2.0 Å are assigned to Cu−Cu and second shell Cu−O single-scattering paths.[72] The appearance of these features is attributed to the formation of the active tricopper-oxo cluster.[7] EXAFS fitting analysis of the Cu-MOR sample after activation in O_2 at 450 °C, including Cu−Al scattering, showed that the intensity of the Cu−Al path is lower compared to that of Cu−Cu (see details in the Supporting Information). Therefore, although we cannot rule out a small contribution of Cu−Al scattering to the feature at ca. 2.3 Å, we attribute the observed

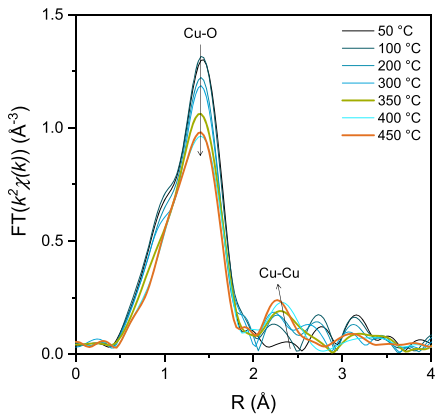

Figure 5. k^2-weighted Fourier-transformed (FT)-EXAFS of the Cu-MOR sample during thermal activation in the O_2 flow with a heating rate of 10 °C/min.

DOI: 10.1021/acs.jpcc.8b10293
J. Phys. Chem. C 2019, 123, 8759−8769

intensity to Cu−Cu single scattering. The decrease of the first shell intensity with increasing temperature is attributed to a decrement of the number of O atoms coordinated to Cu^{2+}. These results indicate a change in the coordination structure of Cu with increasing temperature, in good agreement with XANES (Figure 3) that is attributed to the dehydration of the Cu^{2+}-aquo complex and the formation of tricopper-oxo clusters.

The rdfs of Cu-MOR (Figure 6) measured in situ during thermal activation in He shows the most prominent peak to be

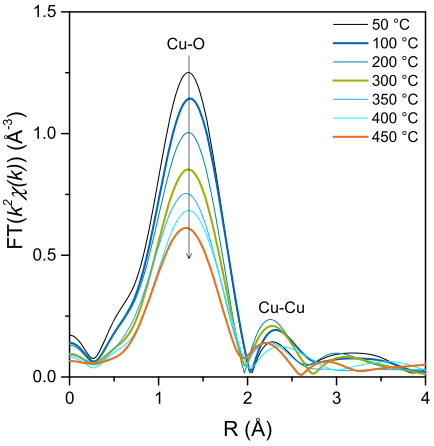

Figure 6. k^2-weighted FT-EXAFS of the Cu-MOR catalyst during thermal activation in He flow with a heating rate of 10 °C/min.

caused by Cu−O back scattering, observed below 2 Å in the *R*-space. With increasing temperature, a distinct peak appears at large interatomic distances ($R \approx 2.3$ Å—not phase corrected) corresponding to the second coordination shell of Cu, which is assigned to a Cu−Cu path.[5,7] This feature can be observed at 100 °C and is attributed to the formation of μ-oxo bridges between Cu^{2+} species. We conclude that it is the result of condensation of two adjacent $[CuOH]^+$ species. This feature remains largely unchanged in intensity up to 300 °C. The intensity of the first shell feature decreased with increasing temperature, indicating a decrease in the number of O atoms coordinated to Cu^{2+}. Both observations are attributed to the dehydration of Cu^{2+}-exchanged species. However, above 300 °C, the intensity of the Cu−Cu path decreased, and it disappeared completely at 400 °C. In the temperature range of 300−450 °C, further decrease of the Cu−O first shell intensity is observed, leading to a final Cu−O coordination number of approximately 2.

In situ XANES showed that dehydration of Cu-MOR is largely complete at 350 °C (Figure 3). Taking into account that a significant fraction of Cu^{2+} is still present at this temperature, it is reasonable to assume the presence of $[Cu-O-Cu]^{2+}$ species formed via condensation of two $[CuOH]^+$ species. It is reported that the autoreduction of such O-bridged Cu species proceeds by desorption and recombination of the bridging oxygen atoms.[35,47−49] Therefore, the further decrease in O coordination in the range of 300−450 °C together with complete reduction of Cu^{2+} to Cu^+, as observed in XANES, is attributed to autoreduction via elimination of O_2 from μ-oxo bridges. Thus, the lower intensity of the Cu−Cu path at temperatures above 300 °C (Figure 5) is likely due to the formation of Cu^+-Cu^+ species that is either stabilized by an Al pair or redispersed across the framework.[40]

Finally, the XANES and EXAFS of Cu-MOR activated in O_2 (1 h) are compared with Cu-MOR activated in He at 450 °C (1 h) followed by oxidation at 200 °C for 15 min (Figures 7 and S9). Both activation treatments have yielded equally active catalysts, as seen in Figure 2. The Cu^+ feature at 8984 eV emerged after activation in He and disappeared completely after exposure to O_2 at 200 °C as well as 450 °C. The XANES obtained after treatment of Cu-MOR at 200 °C for 15 min in O_2 was identical to the one obtained for a sample activated in O_2 at 450 °C for 1 h. Overlapping EXAFS of the Cu-MOR also indicates that the structure of Cu species obtained by both activation treatments can be regarded as identical. Thus, we conclude that a precursor of the trinuclear copper-oxo cluster is formed during treatment at high temperatures (450−500 °C). Given the autoreduction process observed in thermal treatment under an inert atmosphere, such a precursor seems to consist of Cu^+ or a mixture of Cu^+/Cu^{2+} species. The identical structure (Figure 6) and activity in methane oxidation (Figure 2) of Cu species in Cu-MOR samples oxidized at 200 and 450 °C indicate that the trimer precursor is fully reoxidized when contacted with O_2, regardless of the oxidation temperature applied.

The formation of active trinuclear copper-oxo clusters upon contacting the cluster precursor with O_2 has been associated with specific bands in the UV−vis spectra.[7] The in situ UV−vis spectra of Cu-MOR during oxidation of the cluster precursor at 200 °C after activation at 450 °C in the N_2 atmosphere are

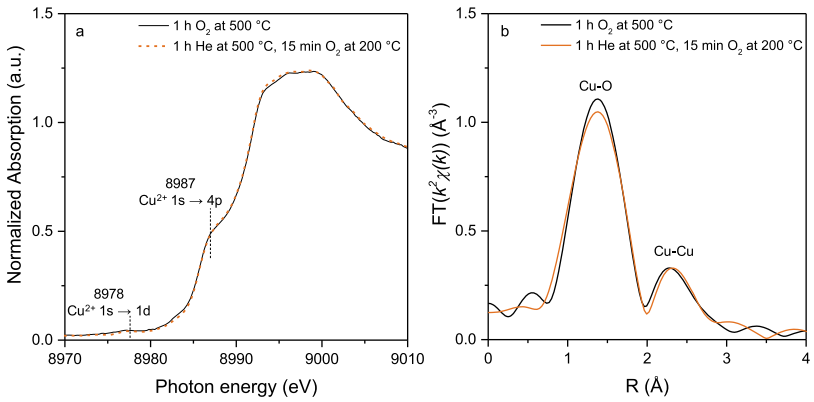

Figure 7. Comparison of (a) Cu K-edge XANES and (b) k^2-weighted FT-EXAFS of Cu-MOR treated at 450 °C in O_2 and Cu-MOR oxidized at 200 °C in O_2 after treatment in He at 450 °C.

DOI: 10.1021/acs.jpcc.8b10293
J. Phys. Chem. C 2019, 123, 8759−8769

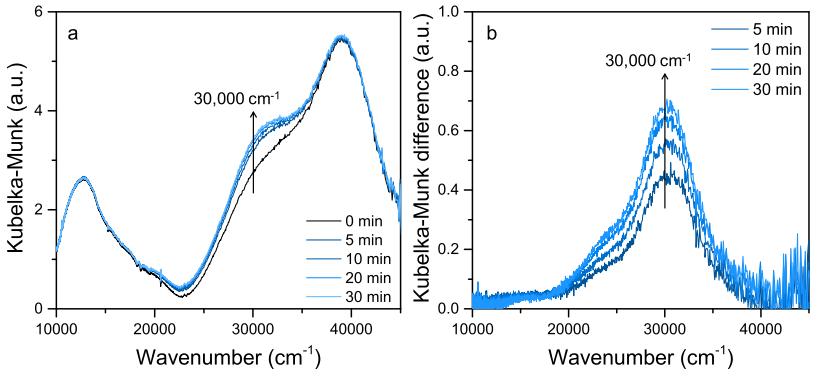

Figure 8. In situ UV−vis spectra of Cu-MOR during activation in O_2 at 200 °C after having been thermally treated in N_2 at 450 °C (a) and the corresponding difference spectra obtained by subtracting the spectrum taken at 0 min (b).

shown in Figure 8. The band observed at ca. 13 000 cm^{-1} and the weak shoulder at ca. 16 500 cm^{-1} are attributed to the d−d transition of Cu^{2+} in square-pyramidal or pyramidal and square-planar coordination structures.[73,74] Previously, we tentatively associated the trinuclear copper-oxo cluster in activated Cu-MOR with a contribution to a broad band at ca. 31 000 cm^{-1} in the UV−vis spectrum because this band was the only one that decreased upon reaction with methane.[7] We have observed that this characteristic band at ca. 30 000 cm^{-1} is weakly present in a N_2-activated Cu-MOR sample, and its intensity increased after contact with O_2 at 200 °C. Inspection of the difference spectra showed a shoulder at 24 000 cm^{-1}, which also increases upon contact with O_2. The low resolution of the spectra, however, does not allow for an assignment of this shoulder to a particular electronic transition. Upon reaction of CH_4 on the oxidized catalyst, a decrease in the intensity of the UV−vis absorption at ca. 30 000 and 38 000 cm^{-1} was observed (Figure S10). These bands are assigned to the $Cu^{2+} \leftarrow O^{2-}$ charge transfer. The band at 30 000 cm^{-1} is associated with $[Cu_3(\mu\text{-}O)_3]^{2+}$.[7] We hypothesize that the band at 38 000 cm^{-1} is also due to this Cu species because the tricopper-oxo cluster contains Cu and O atoms with different electron spin densities.[7,57] This indicates that an active species consistent with a Cu-oxo trimer[7] is formed under oxidative activation of Cu-MOR at low temperatures (200 °C), as long as the material is subjected to a thermal pretreatment in an inert atmosphere at 500 °C.

These results, together with the lack of dependence of the methanol selectivity with temperature or nature of the oxidant (Figures 2 and S3), support the conclusion that the cluster precursor formed at high temperatures can be oxidized in the presence of O_2 or N_2O at lower temperatures (at least 200 °C) to form the active tricopper-oxo cluster.

3.4. Formation of Active $[Cu_3(\mu\text{-}O)_3]^{2+}$ in MOR. Having established that thermal activation of Cu-MOR is essential for the generation of copper-μ-oxo species active in methane oxidation to methanol, we address the pathway for this chemistry. Several mechanisms for the formation of active Cu species during the activation of Cu zeolites have been previously proposed for Cu-ZSM-5,[35] Cu-SSZ-13,[25] and Cu-MOR.[24] Smeets et al.[35] proposed that the active sites in Cu-ZSM-5 are $[Cu(\mu\text{-}O)Cu]^{2+}$ species, with the fingerprint UV−vis band at 22 700 cm^{-1}. According to these authors, a different formation mechanism of active $[Cu(\mu\text{-}O)Cu]^{2+}$ species is verified depending on the nature of the oxidant.

In the present work, differences between oxidation in O_2 and N_2O were not observed either in the yield of CH_4 oxidation or in the selectivity to methanol, as long as the oxidation is preceded by high-temperature pretreatment (Figures 2 and S3). Thus, we conclude that the cleavage of the O−O bond in molecular O_2 is not kinetically or thermodynamically limiting and occurs close to ambient temperature to form active $[Cu_3(\mu\text{-}O)_3]^{2+}$ clusters in MOR. This conclusion, however, may not necessarily be transferable to other zeolite frameworks in view of the different behavior reported for Cu-ZSM-5 and Cu-SSZ-13 by other authors.[25,35] Differences in Cu speciation with the zeolite framework have been widely reported before,[7,25,34] and it is therefore not surprising that the processes involved here in the formation of Cu-oxo species active in methane oxidation also follow different mechanisms.

Our results indicate that the necessity of high-temperature treatment (in either inert or oxidant atmosphere) to achieve a high catalytic activity in Cu-MOR must be related to steps preceding the (re)oxidation of the precursor of the Cu active species. In situ XAS (Figure 3) showed that the transformation of the octahedral Cu^{2+} complexes in the zeolite pores into dehydrated and framework-coordinated Cu^{2+} was largely complete at 350 °C. However, when Cu-MOR was activated at 350 °C in O_2, it only reached 54% of the full activity (achieved at 500 °C in O_2). Hence, we hypothesize that dehydration is not the sole reason for high-temperature activation. Above 350 °C in an inert atmosphere, the majority of Cu^{2+} was concluded to be reduced to Cu^+ (Figure 4), partly even during activation in O_2 (Figure 3). We hypothesize that the appearance of Cu^+ in samples treated at high temperatures is due to the reversible emission of O from μ-oxo bridges between Cu^{2+} species. Such a reaction equilibrium would be shifted toward the desorption of O as O_2 at increasing temperatures. Small concentrations of Cu^+ were observed during activation in O_2, which indicate that the autoreduction reaction is feasible in the presence of oxygen, even though the equilibrium is shifted toward higher concentrations of Cu^{2+} species. The stabilization of Cu^+ species provided by the localized negative charges of the zeolite[75,76] could explain the presence of Cu^+ in spite of being thermodynamically not favored.

Studies on Cu speciation in Cu-SSZ-13 have shown a higher mobility of Cu^+ compared to Cu^{2+} because of the weaker ionic interactions of monovalent Cu^+ with the negatively charged zeolite framework.[45] In line with this conclusion, Hall and Li speculated that the reduction of Cu^{2+} to Cu^+ facilitated redistribution of Cu and therefore enhanced the formation of active sites in Cu-ZSM-5.[52] Recently, both reduction of Cu^{2+} to Cu^+ and migration of Cu cations to 6*R* of the CHA

DOI: 10.1021/acs.jpcc.8b10293
J. Phys. Chem. C 2019, 123, 8759−8769

structure at temperatures above 375 °C were observed for Cu-SSZ-13.[44] Thus, the formation of a mobile Cu^+ species is hypothesized to facilitate the redistribution and migration of Cu in MOR. The lower concentration of active sites in Cu-MOR, activated in He at 350 °C and subsequently oxidized at 200 °C in O_2 (Figure 2), is attributed to limited mobility or a limited concentration of Cu^+. Conversely, activation at 450–500 °C provides the conditions for a larger concentration of Cu^+ to form the precursor of active Cu-oxo clusters.

On the basis of the results obtained here, we propose that formation of the active Cu-μ-oxo cluster occurs via the series of elementary steps shown in Scheme 1. The scheme is valid for

Scheme 1. Reaction Steps Proposed for the Formation of Tricopper-oxo Clusters in Cu-MOR[a]

$$(Z^-)_2[Cu^{II}(H_2O)_n]^{2+} \rightleftharpoons Z^-[Cu^{II}(H_2O)_{n-1}OH]^+ + Z^-H^+ \quad (4.1)$$

$$Z^-[Cu(H_2O)_{n-1}OH]^+ \rightleftharpoons Z^-[Cu^{II}OH]^+_{AlF} + (n-1)\,H_2O \quad (4.2)$$

$$2Z^-[Cu\text{-}OH]^+_{AlF} \longrightarrow (Z^-)_2[Cu^{II}\text{-}O\text{-}Cu^{II}]^{2+}_{2AlF} + H_2O \quad (4.3)$$

$$(Z^-)_2[Cu^{II}\text{-}O\text{-}Cu^{II}]^{2+}_{2AlF} \rightleftharpoons 2(Z^-Cu^+_{AlF}) + 1/2\,O_2 \quad (4.4a)$$

$$Z^-[Cu^{II}OH]_{AlF} \rightleftharpoons Z^-Cu^+_{AlF} + \bullet OH \quad (4.4b)$$

$$2(Z^-Cu^+_{AlF}) + Z^-Cu^+_{mig} + O_2 + \bullet OH \longrightarrow (Z^-)_2[Cu^{II}_3(\mu\text{-}O)_3]^{2+}_{2AlF} + Z^-H^+ \quad (4.5a)$$

$$(Z^-)_2[Cu^{II}\text{-}O\text{-}Cu^{II}]^{2+}_{2AlF} + Z^-Cu^+_{mig} + 1/2\,O_2 + \bullet OH \longrightarrow (Z^-)_2[Cu^{II}_3(\mu\text{-}O)_3]^{2+}_{2AlF} + Z^-H^+ \quad (4.5b)$$

[a] Z^- stands for a negatively charged Al–O^-–Si site of the zeolite framework. "AlF" indicates the cationic species coordinated to the negatively charged framework Al sites of MOR, and "mig" indicates migrated cationic species.

the formation of the active cluster from fresh and spent Cu-MOR samples in a hydrated form. First, the exchange of Cu^{2+} species in aqueous solution can take place either in Al pairs or in one isolated Al T-site of the zeolite. At the moderate pH used in this study, partial dissociation of water ligands takes place, and ion exchange occurs also via the Hirschler–Plank-mechanism in the zeolite pores leading to $(Cu–OH)^+$ (reaction 4.1).[61,77] Then, as seen by XAS (Figures 4 and 6), Cu^{2+} species is dehydrated when the temperature is increased, resulting in a change of coordination from the octahedral to framework-coordinated $[Cu^{II}OH]^+$ species (reaction 4.2). The formation of μ-oxo bridges occurs via condensation of two adjacent $[Cu^{II}OH]^+$ species (reaction 4.3)[43] in the temperature range of 50–300 °C (Figure 6). At 450 °C, significant concentrations of Cu^{2+} have been auto-reduced to Cu^+ (although formation of first Cu^+ species can be detected already at 200 °C). This autoreduction is hypothesized to involve the emission of O_2 from the Cu–O–Cu μ-oxo bridges (reaction 4.4a).[43] The autoreduction of $[Cu^{II}OH]^+$ has been also proposed to take place by the formation of a OH radical from the OH ligand,[42,50] leading to Cu^+ species coordinated to isolated Al-sites (reaction 4.4b).

Larsen et al. proposed that the OH radical species generated in reaction 4.4b decompose by reaction with a second $[CuOH]^+$, releasing H_2O and forming a $Cu^{2+}O^-$ species.[50] Such a scheme implies the mobilization of OH radicals to a second Cu ion in the framework. However, if Cu^+ formed in reaction 4.4b is mobilized above 400 °C, the local negative charge of the zeolite framework left behind needs to be compensated. We speculate that the OH radical species may decompose into a H^+—compensating a negative charge at the Al T-site—and an O^- species. In the next step, the Cu^+ mobile species reacts with Cu pairs located at Al pairs and are reoxidized to Cu^{2+} by a combination of O_2 (or N_2O) and the generated O^- species, leading to the active $[Cu^{II}_3(\mu\text{-}O)_3]^{2+}$ cluster. Taking into account the Al distribution for the present MOR under study, with a high concentration of Al sites in 8-MR positions,[7] it is to be expected that Cu pairs are located in 8-MR, whereas the Cu^+ mobile species originates in isolated exchanged sites in the 12-MR channels.

Two possible pathways for the overall reaction of formation of the oxidized cluster are shown in reactions 4.5a and b. As mentioned above, previous characterization of Cu-MOR has shown that Cu-oxo species are preferentially located at the pore mouth of 8 MR side pockets of MOR because such framework positions are often multiple Al-substituted.[7] Therefore, it is reasonable to expect the presence of species such as those proposed in reaction 4.5a, $[Cu^{II}–O–Cu^{II}]^{2+}–2Al_F$ species, or in reaction 4.5b, $Cu^+–Cu^+$ (which is the reduced analog of $[Cu^{II}–O–Cu^{II}]^{2+}$) at the 8 MR side pocket of MOR.

The experiments emphasize the necessity of a thermal treatment inducing the formation of the mobile species via reaction 4.4. Nearly full activity of Cu-MOR was reached after oxidation at low temperatures of a He-activated sample (Figure 2). Thus, the last step in the mechanism of formation of the active Cu-oxo cluster (any of the alternative reactions 4.5) has a high driving force in the presence of O_2 or N_2O and occurs to near completion already at 50 °C. This is confirmed by the observation that the rdf and XANES (Figure 7) of Cu species after high-temperature and low-temperature oxidations were identical.

4. CONCLUSIONS

The formation of Cu-μ-oxo species in Cu^{2+}-exchanged MOR was shown to occur through a combination of thermal activation of the cationic species followed by an oxidation step. XAS demonstrated that dehydration of the octahedral Cu^{2+} complexes leads to μ-oxo bridged Cu^{2+} species coordinated to framework Al sites in the temperature range of 50–300 °C. Formation of Cu^+ occurs by autoreduction via thermally driven emission of the Cu–O–Cu bridging oxygen and/or by the generation of OH radicals from $[CuOH]^+$. The autoreduction starts at 200 °C in an inert atmosphere but reaches its maximum only at 450–500 °C. It is unclear at present to what extent this reduction is required to induce cation mobility. We hypothesize that the high mobility of Cu^+ is essential to enable the reorganization of Cu ions to form a precursor of the active multicopper cluster. The last step is the oxidation of this precursor to form the active (tri)nuclear copper-oxo cluster, which takes place under mild conditions (50–200 °C) in the presence of strong oxidants such as O_2 or N_2O. The fact that Cu speciation in MOR micropores seems to be significantly different from Cu in ZSM-5 or SSZ-13 highlights the critical role of a specific zeolite lattice. The high efficiency of MOR in forming active Cu-oxo clusters even at low oxidation temperatures is attributed to a high concentration of Al pairs at the pore mouth of the 8 MR side pocket of MOR, which is a position structurally accessible for the formation of Cu-oxo clusters. Although the present study highlights the importance of individual steps in the formation of the active species, more work is needed to understand how aluminum siting and structural aspects of zeolite lattice can be used to direct and maximize the concentration of the active sites.

DOI: 10.1021/acs.jpcc.8b10293
J. Phys. Chem. C 2019, 123, 8759–8769

■ ASSOCIATED CONTENT

Supporting Information

The Supporting Information is available free of charge on the ACS Publications website at DOI: 10.1021/acs.jpcc.8b10293.

Compositions of parent H-MOR and Cu-MOR samples; in situ IR spectra of Cu-MOR measured while heating up in O_2; yields and selectivities of CH_4 oxidation on Cu-MOR after activation under different conditions; k^2-weighted EXAFS of Cu-MOR during thermal treatment in O_2 and He; EXAFS fitting analysis of Cu-MOR after activation in O_2 at 450 °C using DFT-optimized model structures of Cu clusters; k^2-weighted EXAFS of Cu-MOR after activation under different conditions; and in situ diffuse-reflectance UV−vis spectra of Cu-MOR during reaction with CH_4 (PDF)

■ AUTHOR INFORMATION

Corresponding Authors

*E-mail: m.sanchez@tum.de (M.S.-S.).
*E-mail: johannes.lercher@ch.tum.de (J.A.L.).

ORCID

Andreas Jentys: 0000-0001-5877-5042
Guanna Li: 0000-0003-3031-8119
Evgeny Pidko: 0000-0001-9242-9901
John Fulton: 0000-0001-9361-9803
Johannes A. Lercher: 0000-0002-2495-1404

Notes

The authors declare no competing financial interest.

■ ACKNOWLEDGMENTS

The financial support from the Deutsche Forschungsgemeinschaft DFG under project LE1187/13-1 is acknowledged. Part of the research was supported by the TUM International Graduate School of Science and Engineering (IGSSE) and the Max-Buchner Forschungsstiftung from DECHEMA (grant number 3568). We acknowledge DESY (Hamburg, Germany), a member of the Helmholtz Association HGF, for the provision of experimental facilities. Parts of this research were carried out at PETRA III, and we would like to thank Edmung Welter for assistance in using beamline P 65.

■ REFERENCES

(1) Malakoff, D. The gas surge. *Science* **2014**, *344*, 1464−1467.

(2) Wang, V. C.-C.; Maji, S.; Chen, P. P.-Y.; Lee, H. K.; Yu, S. S.-F.; Chan, S. I. Alkane Oxidation: Methane Monooxygenases, Related Enzymes, and Their Biomimetics. *Chem. Rev.* **2017**, *117*, 8574−8621.

(3) Lieberman, R. L.; Rosenzweig, A. C. Crystal Structure of a Membrane-Bound Metalloenzyme That Catalyses the Biological Oxidation of Methane. *Nature* **2005**, *434*, 177−182.

(4) Merkx, M.; Kopp, D. A.; Sazinsky, M. H.; Blazyk, J. L.; Müller, J.; Lippard, S. J. Dioxygen Activation and Methane Hydroxylation by Soluble Methane Monooxygenase: A Tale of Two Irons and Three Proteins A list of abbreviations can be found in Section 7. *Angew. Chem., Int. Ed.* **2001**, *40*, 2782−2807.

(5) Groothaert, M. H.; van Bokhoven, J. A.; Battiston, A. A.; Weckhuysen, B. M.; Schoonheydt, R. A. Bis(μ-oxo)dicopper in Cu-ZSM-5 and Its Role in the Decomposition of NO: A Combined in Situ XAFS, UV−Vis−Near-IR, and Kinetic Study. *J. Am. Chem. Soc.* **2003**, *125*, 7629−7640.

(6) Alayon, E. M.; Nachtegaal, M.; Ranocchiari, M.; van Bokhoven, J. A. Catalytic Conversion of Methane to Methanol over Cu-Mordenite. *Chem. Commun.* **2012**, *48*, 404−406.

(7) Grundner, S.; Markovits, M. A. C.; Li, G.; Tromp, M.; Pidko, E. A.; Hensen, E. J. M.; Jentys, A.; Sanchez-Sanchez, M.; Lercher, J. A. Single-Site Trinuclear Copper Oxygen Clusters in Mordenite for Selective Conversion of Methane to Methanol. *Nat. Commun.* **2015**, *6*, 7546.

(8) Narsimhan, K.; Iyoki, K.; Dinh, K.; Román-Leshkov, Y. Catalytic Oxidation of Methane into Methanol over Copper-Exchanged Zeolites with Oxygen at Low Temperature. *ACS Cent. Sci.* **2016**, *2*, 424−429.

(9) Mahyuddin, M. H.; Staykov, A.; Shiota, Y.; Yoshizawa, K. Direct Conversion of Methane to Methanol by Metal-Exchanged ZSM-5 Zeolite (Metal = Fe, Co, Ni, Cu). *ACS Catal.* **2016**, *6*, 8321−8331.

(10) Snyder, B. E. R.; Vanelderen, P.; Bols, M. L.; Hallaert, S. D.; Böttger, L. H.; Ungur, L.; Pierloot, K.; Schoonheydt, R. A.; Sels, B. F.; Solomon, E. I. The Active Site of Low-Temperature Methane Hydroxylation in Iron-Containing Zeolites. *Nature* **2016**, *536*, 317−321.

(11) Starokon, E. V.; Parfenov, M. V.; Pirutko, L. V.; Abornev, S. I.; Panov, G. I. Room-Temperature Oxidation of Methane by α-Oxygen and Extraction of Products from the FeZSM-5 Surface. *J. Phys. Chem. C* **2011**, *115*, 2155−2161.

(12) Göltl, F.; Michel, C.; Andrikopoulos, P. C.; Love, A. M.; Hafner, J.; Hermans, I.; Sautet, P. Computationally Exploring Confinement Effects in the Methane-to-Methanol Conversion Over Iron-Oxo Centers in Zeolites. *ACS Catal.* **2016**, *6*, 8404−8409.

(13) Dědeček, J.; Kaucký, D.; Wichterlová, B. Co^{2+} Ion Siting in Pentasil-Containing Zeolites, Part 3.: Co^{2+} Ion Sites and Their Occupation in ZSM-5: a VIS Diffuse Reflectance Spectroscopy Study. *Microporous Mesoporous Mater.* **2000**, *35−36*, 483−494.

(14) Dědeček, J.; Wichterlová, B. Co^{2+} Ion Siting in Pentasil-Containing Zeolites. I. Co^{2+} Ion Sites and Their Occupation in Mordenite. A Vis−NIR Diffuse Reflectance Spectroscopy Study. *J. Phys. Chem. B* **1999**, *103*, 1462−1476.

(15) Vanelderen, P.; Snyder, B. E. R.; Tsai, M.-L.; Hadt, R. G.; Vancauwenbergh, J.; Coussens, O.; Schoonheydt, R. A.; Sels, B. F.; Solomon, E. I. Spectroscopic Definition of the Copper Active Sites in Mordenite: Selective Methane Oxidation. *J. Am. Chem. Soc.* **2015**, *137*, 6383−6392.

(16) de Graaf, J.; van Dillen, A. J.; de Jong, K. P.; Koningsberger, D. C. Preparation of Highly Dispersed Pt Particles in Zeolite Y with a Narrow Particle Size Distribution: Characterization by Hydrogen Chemisorption, TEM, EXAFS Spectroscopy, and Particle Modeling. *J. Catal.* **2001**, *203*, 307−321.

(17) Wang, D.; Lunsford, J. H.; Rosynek, M. P. Characterization of a Mo/ZSM-5 Catalyst for the Conversion of Methane to Benzene. *J. Catal.* **1997**, *169*, 347−358.

(18) Sobolev, V. I.; Kovalenko, O. N.; Kharitonov, A. S.; Pankrat'ev, Y. D.; Panov, G. I. Anomalously Low Bond Energy of Surface Oxygen on FeZSM-5 Zeolite. *Mendeleev Commun.* **1991**, *1*, 29−30.

(19) Groothaert, M. H.; Smeets, P. J.; Sels, B. F.; Jacobs, P. A.; Schoonheydt, R. A. Selective Oxidation of Methane by the Bis(μ-oxo)dicopper Core Stabilized on ZSM-5 and Mordenite Zeolites. *J. Am. Chem. Soc.* **2005**, *127*, 1394−1395.

(20) Sheppard, T.; Hamill, C. D.; Goguet, A.; Rooney, D. W.; Thompson, J. M. A Low Temperature, Isothermal Gas-Phase System for Conversion of Methane to Methanol Over Cu-ZSM-5. *Chem. Commun.* **2014**, *50*, 11053−11055.

(21) Le, H. V.; Parishan, S.; Sagaltchik, A.; Göbel, C.; Schlesiger, C.; Malzer, W.; Trunschke, A.; Schomäcker, R.; Thomas, A. Solid-State Ion-Exchanged Cu/Mordenite Catalysts for the Direct Conversion of Methane to Methanol. *ACS Catal.* **2017**, *7*, 1403−1412.

(22) Oord, R.; Schmidt, J. E.; Weckhuysen, B. M. Methane-to-Methanol Conversion Over Zeolite Cu-SSZ-13, and Its Comparison with the Selective Catalytic Reduction of NOx with NH_3. *Catal. Sci. Technol.* **2018**, *8*, 1028−1038.

(23) Wulfers, M. J.; Teketel, S.; Ipek, B.; Lobo, R. F. Conversion of Methane to Methanol on Copper-Containing Small-Pore Zeolites and Zeotypes. *Chem. Commun.* **2015**, *51*, 4447−4450.

DOI: 10.1021/acs.jpcc.8b10293
J. Phys. Chem. C 2019, 123, 8759−8769

(24) Kim, Y.; Kim, T. Y.; Lee, H.; Yi, J. Distinct Activation of Cu-MOR for Direct Oxidation of Methane to Methanol. *Chem. Commun.* **2017**, *53*, 4116−4119.
(25) Pappas, D. K.; Borfecchia, E.; Dyballa, M.; Pankin, I. A.; Lomachenko, K. A.; Martini, A.; Signorile, M.; Teketel, S.; Arstad, B.; Berlier, G.; Lamberti, C.; Bordiga, S.; Olsbye, U.; Lillerud, K. P.; Svelle, S.; Beato, P. Methane to Methanol: Structure-Activity Relationships for Cu-CHA. *J. Am. Chem. Soc.* **2017**, *139*, 14961−14975.
(26) Pappas, D. K.; Martini, A.; Dyballa, M.; Kvande, K.; Teketel, S.; Lomachenko, K. A.; Baran, R.; Glatzel, P.; Arstad, B.; Berlier, G.; Lamberti, C.; Bordiga, S.; Olsbye, U.; Svelle, S.; Beato, P.; Borfecchia, E. The Nuclearity of the Active Site for Methane to Methanol Conversion in Cu-Mordenite: A Quantitative Assessment. *J. Am. Chem. Soc.* **2018**, *140*, 15270−15278.
(27) Tsai, M.-L.; Hadt, R. G.; Vanelderen, P.; Sels, B. F.; Schoonheydt, R. A.; Solomon, E. I. $[Cu_2O]^{2+}$ Active Site Formation in Cu−ZSM-5: Geometric and Electronic Structure Requirements for N_2O Activation. *J. Am. Chem. Soc.* **2014**, *136*, 3522−3529.
(28) Ipek, B.; Lobo, R. F. Catalytic Conversion of Methane to Methanol on Cu-SSZ-13 Using N_2O as Oxidant. *Chem. Commun.* **2016**, *52*, 13401−13404.
(29) Li, G.; Vassilev, P.; Sanchez-Sanchez, M.; Lercher, J. A.; Hensen, E. J. M.; Pidko, E. A. Stability and Reactivity of Copper Oxo-Clusters in ZSM-5 Zeolite for Selective Methane Oxidation to Methanol. *J. Catal.* **2016**, *338*, 305−312.
(30) Grundner, S.; Luo, W.; Sanchez-Sanchez, M.; Lercher, J. A. Synthesis of Single-Site Copper Catalysts for Methane Partial Oxidation. *Chem. Commun.* **2016**, *52*, 2553−2556.
(31) Markovits, M. A. C.; Jentys, A.; Tromp, M.; Sanchez-Sanchez, M.; Lercher, J. A. Effect of Location and Distribution of Al Sites in ZSM-5 on the Formation of Cu-Oxo Clusters Active for Direct Conversion of Methane to Methanol. *Top. Catal.* **2016**, *59*, 1554−1563.
(32) Alayon, E. M. C.; Nachtegaal, M.; Kleymenov, E.; van Bokhoven, J. A. Determination of the Electronic and Geometric Structure of Cu Sites during Methane Conversion over Cu-MOR with X-ray Absorption Spectroscopy. *Microporous Mesoporous Mater.* **2013**, *166*, 131−136.
(33) Alayon, E. M. C.; Nachtegaal, M.; Bodi, A.; Ranocchiari, M.; van Bokhoven, J. A. Bis(μ-oxo) Versus Mono(μ-oxo)Dicopper Cores in a Zeolite for Converting Methane to Methanol: an In Situ XAS and DFT Investigation. *Phys. Chem. Chem. Phys.* **2015**, *17*, 7681−7693.
(34) Woertink, J. S.; Smeets, P. J.; Groothaert, M. H.; Vance, M. A.; Sels, B. F.; Schoonheydt, R. A.; Solomon, E. I. A $[Cu_2O]^{2+}$ Core in Cu-ZSM-5, The Active Site in the Oxidation of Methane to Methanol. *Proc. Natl. Acad. Sci. U.S.A.* **2009**, *106*, 18908−18913.
(35) Smeets, P. J.; Hadt, R. G.; Woertink, J. S.; Vanelderen, P.; Schoonheydt, R. A.; Sels, B. F.; Solomon, E. I. Oxygen Precursor to the Reactive Intermediate in Methanol Synthesis by Cu-ZSM-5. *J. Am. Chem. Soc.* **2010**, *132*, 14736−14738.
(36) Tomkins, P.; Mansouri, A.; Bozbag, S. E.; Krumeich, F.; Park, M. B.; Alayon, E. M. C.; Ranocchiari, M.; van Bokhoven, J. A. Isothermal Cyclic Conversion of Methane into Methanol over Copper-Exchanged Zeolite at Low Temperature. *Angew. Chem., Int. Ed.* **2016**, *55*, 5467−5471.
(37) Tomkins, P.; Ranocchiari, M.; van Bokhoven, J. A. Direct Conversion of Methane to Methanol Under Mild Conditions Over Cu-Zeolites and Beyond. *Acc. Chem. Res.* **2017**, *50*, 418−425.
(38) Sushkevich, V. L.; Palagin, D.; Ranocchiari, M.; van Bokhoven, J. A. Selective Anaerobic Oxidation of Methane Enables Direct Synthesis of Methanol. *Science* **2017**, *356*, 523−527.
(39) Dedecek, J.; Sobalik, Z.; Tvaruazkova, Z.; Kaucky, D.; Wichterlova, B. Coordination of Cu Ions in High-Silica Zeolite Matrices - Cu^+ Photoluminescence, IR of NO Adsorbed on Cu^{2+}, and Cu^{2+} ESR Study. *J. Phys. Chem.* **1995**, *99*, 16327−16337.
(40) Dědeček, J.; Wichterlová, B. Role of Hydrated Cu Ion Complexes and Aluminum Distribution in the Framework on the Cu Ion Siting in ZSM-5. *J. Phys. Chem. B* **1997**, *101*, 10233−10240.
(41) Alayon, E. M. C.; Nachtegaal, M.; Bodi, A.; van Bokhoven, J. A. Reaction Conditions of Methane-to-Methanol Conversion Affect the Structure of Active Copper Sites. *ACS Catal.* **2014**, *4*, 16−22.
(42) Borfecchia, E.; Lomachenko, K. A.; Giordanino, F.; Falsig, H.; Beato, P.; Soldatov, A. V.; Bordiga, S.; Lamberti, C. Revisiting the Nature of Cu Sites in the Activated Cu-SSZ-13 Catalyst for SCR Reaction. *Chem. Sci.* **2015**, *6*, 548−563.
(43) Llabrés i Xamena, F. X.; Fisicaro, P.; Berlier, G.; Zecchina, A.; Palomino, G. T.; Prestipino, C.; Bordiga, S.; Giamello, E.; Lamberti, C. Thermal Reduction of Cu^{2+}−Mordenite and Re-oxidation upon Interaction with H_2O, O_2, and NO. *J. Phys. Chem. B* **2003**, *107*, 7036−7044.
(44) Andersen, C. W.; Borfecchia, E.; Bremholm, M.; Jørgensen, M. R. V.; Vennestrøm, P. N. R.; Lamberti, C.; Lundegaard, L. F.; Iversen, B. B. Redox-Driven Migration of Copper Ions in the Cu-CHA Zeolite as Shown by the In Situ PXRD/XANES Technique. *Angew. Chem., Int. Ed.* **2017**, *56*, 10367−10372.
(45) Kwak, J. H.; Varga, T.; Peden, C. H. F.; Gao, F.; Hanson, J. C.; Szanyi, J. Following the Movement of Cu Ions in a SSZ-13 Zeolite During Dehydration, Reduction and Adsorption: A Combined in Situ TP-XRD, XANES/DRIFTS Study. *J. Catal.* **2014**, *314*, 83−93.
(46) Attfield, M. P.; Weigel, S. J.; Cheetham, A. K. On the Nature of Nonframework Cations in a Zeolitic deNO_x Catalyst: Cu-Mordenite. *J. Catal.* **1997**, *170*, 227−235.
(47) Iwamoto, M.; Yahiro, H.; Tanda, K.; Mizuno, N.; Mine, Y.; Kagawa, S. Removal of Nitrogen Monoxide Through a Novel Catalytic Process. 1. Decomposition on Excessively Copper-Ion-Exchanged ZSM-5 Zeolites. *J. Phys. Chem.* **1991**, *95*, 3727−3730.
(48) Valyon, J.; Hall, W. K. Effects of Reduction and Reoxidation on the Infrared Spectra from Cu-Y and Cu-ZSM-5 Zeolites. *J. Phys. Chem.* **1993**, *97*, 7054−7060.
(49) Sárkány, J.; d'Itri, J. L.; Sachtler, W. M. H. Redox Chemistry in Excessively Ion-Exchanged Cu/Na-ZSM-5. *Catal. Lett.* **1992**, *16*, 241−249.
(50) Larsen, S. C.; Aylor, A.; Bell, A. T.; Reimer, J. A. Electron Paramagnetic Resonance Studies of Copper Ion-Exchanged ZSM-5. *J. Phys. Chem.* **1994**, *98*, 11533−11540.
(51) Jacobs, P. A.; de Wilde, W.; Schoonheydt, R. A.; Uytterhoeven, J. B.; Beyer, H. Redox Behaviour of Transition Metal Ions in Zeolites. Part 3. Auto-Reduction of Cupric Ions in Y Zeolites. *J. Chem. Soc., Faraday Trans.* **1976**, *72*, 1221.
(52) Li, Y.; Hall, W. K. Catalytic Decomposition of Nitric Oxide over Cu-Zeolites. *J. Catal.* **1991**, *129*, 202−215.
(53) Larsen, S. C.; Aylor, A.; Bell, A. T.; Reimer, J. A. Electron Paramagnetic Resonance Studies of Copper Ion-Exchanged ZSM-5. *J. Phys. Chem.* **1994**, *98*, 11533−11540.
(54) Lei, G. D.; Adelman, B. J.; Sárkány, J.; Sachtler, W. M. H. Identification of Copper(II) and Copper(I) and Their Interconversion in Cu/ZSM-5 De-NOx Catalysts. *Appl. Catal., B* **1995**, *5*, 245−256.
(55) Palomino, G. T.; Fisicaro, P.; Bordiga, S.; Zecchina, A.; Giamello, E.; Lamberti, C. Oxidation States of Copper Ions in ZSM-5 Zeolites. A Multitechnique Investigation. *J. Phys. Chem. B* **2000**, *104*, 4064−4073.
(56) Mahyuddin, M. H.; Tanaka, T.; Shiota, Y.; Staykov, A.; Yoshizawa, K. Methane Partial Oxidation over $[Cu_2(\mu\text{-}O)]^{2+}$ and $[Cu_3(\mu\text{-}O)_3]^{2+}$ Active Species in Large-Pore Zeolites. *ACS Catal.* **2018**, *8*, 1500−1509.
(57) Vogiatzis, K. D.; Li, G.; Hensen, E. J. M.; Gagliardi, L.; Pidko, E. A. Electronic Structure of the $[Cu_3(\mu\text{-}O)_3]^{2+}$ Cluster in Mordenite Zeolite and Its Effects on the Methane to Methanol Oxidation. *J. Phys. Chem. C* **2017**, *121*, 22295−22302.
(58) Ravel, B.; Newville, M. ATHENA,ARTEMIS,HEPHAESTUS: Data Analysis for X-ray Absorption Spectroscopy Using IFEFFIT. *J. Synchrotron Radiat.* **2005**, *12*, 537−541.
(59) Kresse, G.; Furthmüller, J. Efficient Iterative Schemes for ab Initio Total-Energy Calculations Using a Plane-Wave Basis Set. *Phys. Rev. B: Condens. Matter Mater. Phys.* **1996**, *54*, 11169−11186.

DOI: 10.1021/acs.jpcc.8b10293
J. Phys. Chem. C 2019, 123, 8759−8769

(60) Perdew, J. P.; Burke, K.; Ernzerhof, M. Generalized Gradient Approximation Made Simple. *Phys. Rev. Lett.* **1996**, *77*, 3865−3868.
(61) Blöchl, P. E. Projector Augmented-Wave Method. *Phys. Rev. B: Condens. Matter Mater. Phys.* **1994**, *50*, 17953−17979.
(62) Pidko, E. A.; van Santen, R. A.; Hensen, E. J. M. Multinuclear Gallium-Oxide Cations in High-Silica Zeolites. *Phys. Chem. Chem. Phys.* **2009**, *11*, 2893−2902.
(63) Dietl, N.; Schlangen, M.; Schwarz, H. Thermal Hydrogen-Atom Transfer from Methane: The Role of Radicals and Spin States in Oxo-Cluster Chemistry. *Angew. Chem., Int. Ed.* **2012**, *51*, 5544−5555.
(64) Siahrostami, S.; Falsig, H.; Beato, P.; Moses, P. G.; Nørskov, J. K.; Studt, F. Exploring Scaling Relations for Chemisorption Energies on Transition-Metal-Exchanged Zeolites ZSM-22 and ZSM-5. *ChemCatChem* **2016**, *8*, 767−772.
(65) Lo Jacono, M.; Fierro, G.; Dragone, R.; Feng, X.; d'Itr, J.; Hall, W. K. Zeolite Chemistry of CuZSM-5 Revisited. *J. Phys. Chem. B* **1997**, *101*, 1979−1984.
(66) Fanning, P. E.; Vannice, M. A. A DRIFTS Study of Cu−ZSM-5 Prior to and During Its Use for N_2O Decomposition. *J. Catal.* **2002**, *207*, 166−182.
(67) Da Costa, P.; Modén, B.; Meitzner, G. D.; Lee, D. K.; Iglesia, E. Spectroscopic and Chemical Characterization of Active and Inactive Cu Species in NO Decomposition Catalysts Based on Cu-ZSM5. *Phys. Chem. Chem. Phys.* **2002**, *4*, 4590−4601.
(68) Kuroda, Y.; Yoshikawa, Y.; Konno, S.-i.; Hamano, H.; Maeda, H.; Kumashiro, R.; Nagao, M. Specific Feature of Copper Ion-Exchanged Mordenite for Dinitrogen Adsorption at Room Temperature. *J. Phys. Chem.* **1995**, *99*, 10621−10628.
(69) Jang, H.-J.; Hall, W. K.; d'Itri, J. L. Redox Behavior of CuZSM-5 Catalysts: FTIR Investigations of Reactions of Adsorbed NO and CO. *J. Phys. Chem.* **1996**, *100*, 9416−9420.
(70) Nachtigallová, D.; Nachtigall, P.; Sauer, J. Coordination of Cu^+ and Cu^{2+} Ions in ZSM-5 in the Vicinity of Two Framework Al Atoms. *Phys. Chem. Chem. Phys.* **2001**, *3*, 1552−1559.
(71) Gao, F.; Washton, N. M.; Wang, Y.; Kollár, M.; Szanyi, J.; Peden, C. H. F. Effects of Si/Al Ratio on Cu/SSZ-13 NH_3-SCR Catalysts: Implications for the Active Cu Species and the Roles of Brønsted Acidity. *J. Catal.* **2015**, *331*, 25−38.
(72) Tromp, M.; van Bokhoven, J. A.; Arink, A. M.; Bitter, J. H.; van Koten, G.; Koningsberger, D. C. Cu K-Edge EXAFS Characterisation of Copper(I) Arenethiolate Complexes in both the Solid and Liquid State: Detection of Cu−Cu Coordination. *Chem.—Eur. J.* **2002**, *8*, 5667−5678.
(73) Vanelderen, P.; Vancauwenbergh, J.; Tsai, M.-L.; Hadt, R. G.; Solomon, E. I.; Schoonheydt, R. A.; Sels, B. F. Spectroscopy and Redox Chemistry of Copper in Mordenite. *ChemPhysChem* **2014**, *15*, 91−99.
(74) Delabie, A.; Pierloot, K.; Groothaert, M. H.; Weckhuysen, B. M.; Schoonheydt, R. A. The Siting of Cu(II) in Mordenite: a Theoretical Spectroscopic Study. *Phys. Chem. Chem. Phys.* **2002**, *4*, 134−145.
(75) Schoonheydt, R. A. Transition Metal Ions in Zeolites: Siting and Energetics of Cu^{2+}. *Catal. Rev.* **1993**, *35*, 129−168.
(76) Kefirov, R.; Penkova, A.; Hadjiivanov, K.; Dzwigaj, S.; Che, M. Stabilization of Cu^+ Ions in BEA Zeolite: Study by FTIR Spectroscopy of Adsorbed CO and TPR. *Microporous Mesoporous Mater.* **2008**, *116*, 180−187.
(77) Hirschler, A. The Measurement of Catalyst Acidity Using Indicators Forming Stable Surface Carbonium Ions. *J. Catal.* **1963**, *2*, 428−439.

DOI: 10.1021/acs.jpcc.8b10293
J. Phys. Chem. C 2019, 123, 8759−8769